

# Left ventricular epicardial admittance measurement for detection of acute LV dilation

John E. Porterfield,<sup>1</sup> Erik R. Larson,<sup>1</sup> James T. Jenkins,<sup>2,3</sup> Daniel Escobedo,<sup>2,3</sup> Jonathan W. Valvano,<sup>1</sup> John A. Pearce,<sup>1</sup> and Marc D. Feldman<sup>2,3</sup>

<sup>1</sup>The University of Texas at Austin, Austin; and <sup>2</sup>The University of Texas Health Science Center, and <sup>3</sup>Department of Veterans Affairs, South Texas Veterans Health Care System, San Antonio, Texas

Submitted 7 September 2010; accepted in final form 3 December 2010

**Porterfield JE, Larson ER, Jenkins JT, Escobedo D, Valvano JW, Pearce JA, Feldman MD.** Left ventricular epicardial admittance measurement for detection of acute LV dilation. *J Appl Physiol* 110: 799–806, 2011. First published December 9, 2010; doi:10.1152/jappphysiol.01047.2010.— There are two implanted heart failure warning systems incorporated into biventricular pacemakers/automatic implantable cardiac defibrillators and tested in clinical trials: right heart pressures, and lung conductance measurements. However, both warning systems postdate measures of the earliest indicator of impending heart failure: left ventricular (LV) volume. There are currently no proposed implanted technologies that can perform LV blood volume measurements in humans. We propose to solve this problem by incorporating an admittance measurement system onto currently deployed biventricular and automatic implantable cardiac defibrillator leads. This study will demonstrate that an admittance measurement system can detect LV blood conductance from the epicardial position, despite the current generating and sensing electrodes being in constant motion with the heart, and with dynamic removal of the myocardial component of the returning voltage signal. Specifically, in 11 pigs, it will be demonstrated that 1) a physiological LV blood conductance signal can be derived; 2) LV dilation in response to dose-response intravenous neosynephrine can be detected by blood conductance in a similar fashion to the standard of endocardial crystals when admittance is used, but not when only traditional conductance is used; 3) the physiological impact of acute left anterior descending coronary artery occlusion and resultant LV dilation can be detected by blood conductance, before the anticipated secondary rise in right ventricular systolic pressure; and 4) a pleural effusion simulated by placing saline outside the pericardium does not serve as a source of artifact for blood conductance measurements.

early detection of heart failure; bioimpedance; left ventricular preload; end-diastolic volume; conductance

CONDUCTANCE MEASUREMENTS HAVE been available as an invasive tool to detect instantaneous left ventricular (LV) volume since 1981 (2). Tetrapolar electrodes are usually placed on a catheter located within the LV chamber to determine instantaneous volume by electrical conductance measurement. Conductance systems generate an electric field using a current source, and volume is determined from the instantaneous returning voltage signal. Conductance is the preferred measurement over resistance (or impedance), because it has a direct (not inverse) relationship with volume. However, this approach cannot be translated into an implanted device in patients, particularly those with heart failure (HF) where there is clinical need, due

to the risk of stroke. One solution would be to move these electrodes to the LV epicardium, eliminating the risk of stroke.

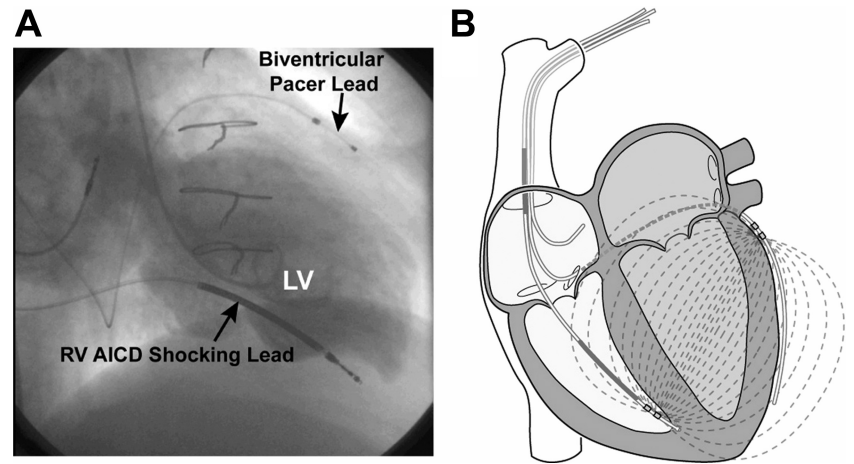
Electrodes have not been previously placed on the LV epicardium to interrogate LV blood volume, as proposed for the first time in the present study. The epicardial location introduces new complexities, including greater contamination of the resulting voltage signal with myocardium when only the LV blood volume is desired. We are able to solve this problem with the use of admittance (the inverse of complex impedance), because admittance is a complex plane number containing information about the permittivity of muscle, which allows separation of the amount of blood and muscle in the signal.

One clinical application of the LV epicardial location would be HF patients. HF is one of the leading causes of admission to the hospital (6). Studies have shown that HF patients with dilated hearts have a reduction in the frequency of hospital admission and prolongation of life with the implantation of biventricular pacemakers and automatic implantable cardiac defibrillators (AICDs) (5, 9, 11, 20). These benefits extend to the millions of patients with both ischemic and idiopathic cardiomyopathy. Recently, technology used in combination with AICDs and biventricular pacemakers for sensing the progression of impending HF to reduce the number and length of stay of hospital admissions for congestive HF has been proposed (1, 10, 18, 19, 27, 28, 31, 32, 35). There are two incorporated HF warning systems used with biventricular pacemakers and AICDs that have been tested in clinical trials. First, Chronicle detects an increase in right heart pressures in an attempt to detect the onset of HF (1, 10, 19). Second, Optivol and CorVue use lung conductance measurements as an indication of pulmonary edema (18, 31, 32, 35). However, both are measures that occur later than the best indicator of impending HF: LV preload.

More recently, Stahl et al. (28, 29) have proposed generating an electric field in the right ventricle (RV), and detecting the fringe field from the LV biventricular pacer lead. However, this measurement does not separate the lumped blood (real) and myocardial (real and imaginary) components of admittance. There are currently no proposed implanted technologies that can perform LV blood volume measurements. We propose to solve this problem by incorporating the admittance measurement system, developed by our group (13, 22–24, 26, 33, 34), onto biventricular and AICD leads, and removing the myocardial contribution from the combined electrical blood/muscle signal to determine an increase in LV preload from baseline. Biventricular leads are already located in ideal measurement locations: the lateral LV epicardium and the RV apex (Fig. 1A). Since blood has five times lower resistivity than myocardium,

Address for reprint requests and other correspondence: M. D. Feldman, Univ. of Texas Health Science Center, Rm. 5.642, 7703 Floyd Curl Dr., San Antonio, TX 78248 (e-mail: feldmanm@uthscsa.edu).

Fig. 1. A: biplane left ventriculogram from a patient with congestive heart failure and a previously implanted automatic implantable cardiac defibrillator (AICD)/biventricular pacer, demonstrating how the leads span the left ventricle (LV) blood from the right ventricle (RV) apical septum to the lateral LV epicardium. B: the admittance electric field lines from the RV apical septum to the lateral LV epicardium.



the preferential path for a substantial fraction of the current flow is the LV blood volume (Fig. 1B).

We demonstrate the validity of our approach by 1) deriving real-time LV blood conductance signals following instantaneous removal of the myocardial component of the signal utilizing epicardial electrodes; 2) detecting LV dilation with blood conductance in response to IV neosynephrine comparable to the standard of endocardial crystals (see Figs. 2 and 3); 3) detecting LV dilation with blood conductance in response to occlusion of the left anterior descending coronary artery (LAD), while RV pressures remain unchanged; and 4) demonstrating that saline placed in the chest cavity to simulate a pleural effusion is not a source of artifact in the measurement of epicardial admittance.

## METHODS

### Calculation Theory

**Epicardial blood conductance measurement.** The relationship between measured blood conductance and LV blood volume is determined primarily by the shape of the current field in the blood pool and surrounding myocardium. For example, in a uniform electric field approximation, the measured time-dependent resistance,  $R_{\text{blood}}$ , is

proportional to the electrode separation distance,  $L(t)$ , and inversely proportional to the cross-sectional area of the field,  $A(t)$ , and the converse for the measured blood conductance,  $G_{\text{blood}}$ , where  $\rho$  is blood resistivity:

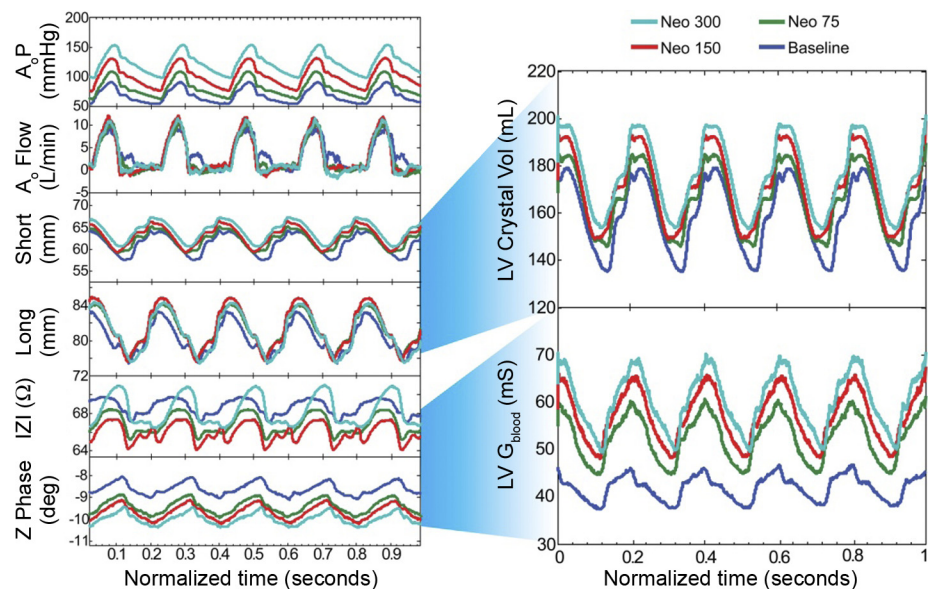
$$R_{\text{blood}} = \frac{\rho L(t)}{A(t)}$$

$$G_{\text{blood}} = \frac{A(t)}{\rho L(t)}$$

Some of the measurement electrode positions will produce a  $G_{\text{blood}}$  primarily sensitive to the cross-sectional area change, while others are primarily sensitive to the separation distance. As the cross-sectional area of the LV increases, there is a corresponding increase in  $G_{\text{blood}}$ . Thus, for the purposes of the present study, we focused on area-dependent electrode configurations only.

**Dynamic muscle conductance removal.** Epicardial admittance is a measurement taken in the complex plane and has both a magnitude,  $|Y|$  (Siemens), and a phase,  $\angle Y$  (degrees). The values for admittance are a combination of both the muscle and  $G_{\text{blood}}$  ( $G$ ), and the muscle susceptance ( $\omega C$ ), for both are present in the current field. The process for separating admittance into blood and muscle conductance was outlined previously for the case of a tetrapolar catheter where the blood and muscle are in parallel (22). However, there is no previously

Fig. 2. Typical neosynephrine (Neo) dose-response (D-R) data obtained from a single porcine study, which demonstrates the raw signals and which signals are used to derive final LV blood conductance ( $G_{\text{blood}}$ ). The aortic (Ao) pressure (P) increased with the Neo D-R, while Ao flow was constant. Both short- and long-axis LV endocardial crystals increased in distance with Neo D-R, as did calculated LV volume (LV Crystal Vol, mL). The epicardial impedance ( $Z$ ) and phase angle ( $Z$  Phase) also changed in response to the Neo D-R, as did calculated LV  $G_{\text{blood}}$  (mS), similar to the LV volume standard (see Fig. 3). Neo 75, 150, and 300 are in units of  $\mu\text{g}/\text{min}$ .



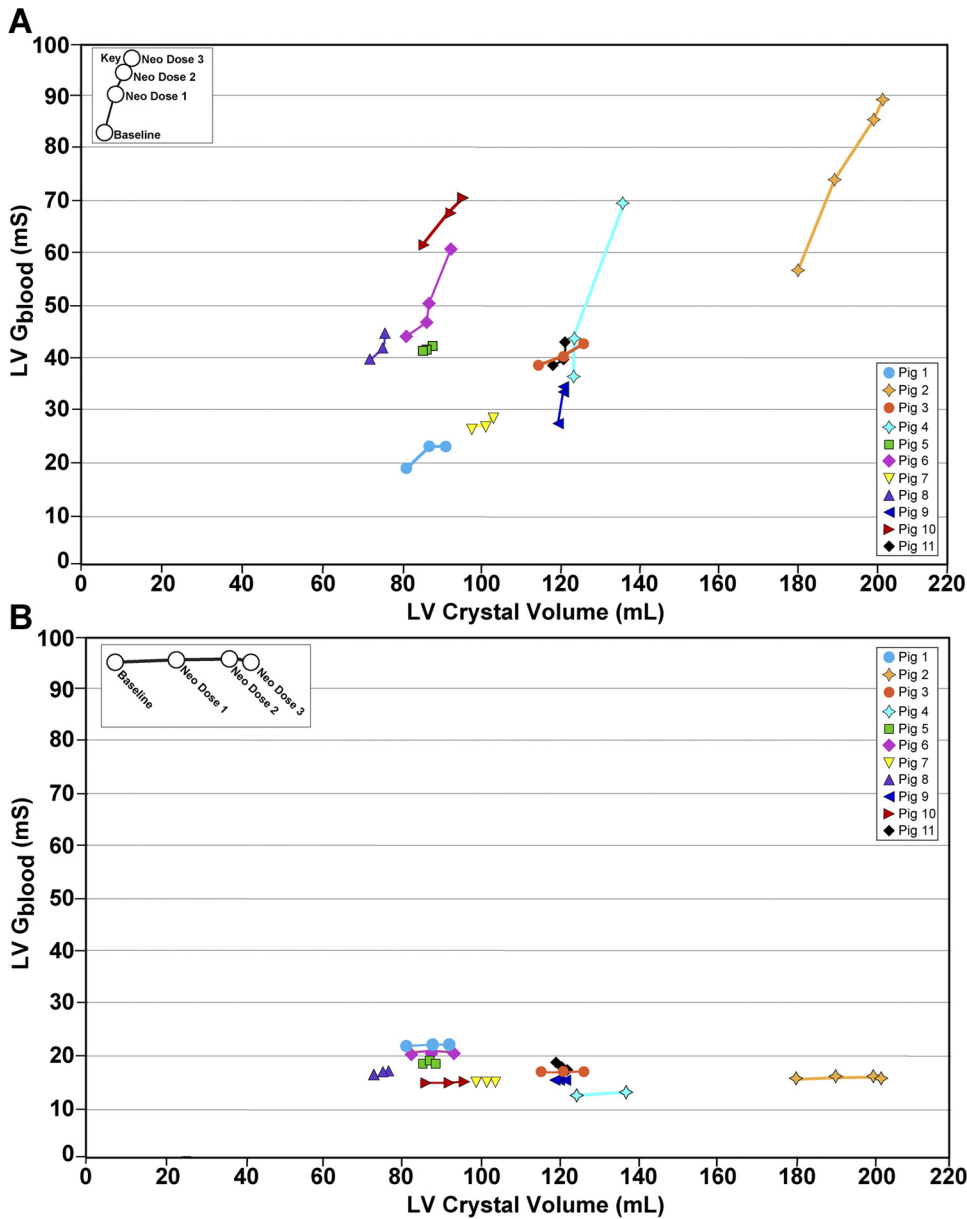


Fig. 3. A: effect of Neo on LV end-diastolic volume in epicardial lead studies. Note that LV  $G_{\text{blood}}$  tracks with the standard of LV crystal volume. B: the same data analyzed without subtracting the muscle component, demonstrating that dynamic removal of the myocardial signal using admittance is critical for detecting increasing LV volume. The pig number is identified in the legend. There is variation in the absolute volumes in these hearts due to a large variation in porcine size.

proposed model for the separation of blood and muscle components of a cross-chamber epicardial admittance measurement, where the blood and muscle components are in series. This new theory to separate blood and muscle components is presented below.

$$R_m = \frac{-\text{Im}\{\bar{Z}\} \times \left[ 1 + \left( \frac{\omega \epsilon_m}{\sigma_m} \right)^2 \right]}{\frac{\omega \epsilon_m}{\sigma_m}}$$

$$R_b = \text{Re}\{\bar{Z}\} - \frac{R_m}{1 + \left( \frac{\omega \epsilon_m}{\sigma_m} \right)^2}$$

Where  $R_m$  is the resistance of muscle ( $\Omega$ ), and  $R_b$  is the resistance of blood ( $\Omega$ ),  $\epsilon_m$  is the permittivity of muscle (F/m), and  $\sigma_m$  is the conductivity of muscle (S/m). The derivations for the above formula are in the attached APPENDIX, and use impedance  $\bar{Z}$  (the inverse of

admittance  $\bar{Y}$ ) because of the ease of mathematical formulation. The complex impedance  $\bar{Z}$  can be separated into real ( $\text{Re}\{\bar{Z}\}$ ) and imaginary parts ( $\text{Im}\{\bar{Z}\}$ ). The properties of the myocardium  $\sigma_m$  and  $\epsilon_m$  can be calculated using a surface probe measurement (22, 24). In an epicardial measurement, the field generated is mostly transverse, while, in a surface probe measurement (and in a traditional LV catheter measurement), the field is mostly longitudinal. This difference has been measured by others and was corrected in our data by multiplying by a factor of 2 (12, 30). The penetration depth for the surface probe used to measure the porcine myocardial properties was 3.6 mm, which does not extend into the LV blood volume beneath.

*LV volume measurement with two-dimensional sonomicrometry.* The standard of volume measurement used in this study is two-dimensional (2D) sonomicrometry (endocardial) crystals. 2D endocardial crystals are an acceptable alternative in large-animal hearts when the two short axes are equal in distance (14, 16, 17), and this distance is maintained during acute LV dilation. The porcine myocardium is prone to arrhythmias, and there is significant trauma

associated with placing the third crystal plane through the septum. Consequently, 2D endocardial crystals are the practical approach. The two dimensions measured included the anterior-posterior and apex-base planes via pairs of 2-mm piezo-electric ultrasonic transducers positioned on the endocardial surface through a stab wound through the LV myocardium and secured with a purse-string suture. The two crystal pairs were attached to a digital sonomicrometer (Sonometrics, London, Ontario, Canada), and the digital output was then transformed into volume by fitting the points to a prolate ellipsoid (14, 17).

### Experimental Protocol

This study was conducted in compliance with the United States Food and Drug Administration Good Laboratory Practices Regulations (21 CFR Part 58), following approval of the animal use committee at the University of Texas Health Science Center San Antonio. For the 15 Yorkshire pigs studied, the body weight ranged from 42 to 78 kg (mean =  $60 \pm 12.6$  kg); 14 were male and 1 was female. Pigs were sedated with Telazol 4 mg/kg im and intubated, and anesthesia was maintained with 1–2% isoflurane with 100% oxygen. The right neck was dissected to gain access to the jugular vein and carotid artery. A sternotomy was performed, and the pericardium was partially opened. Amiodarone at a dose of 150 mg iv was given over 30 min and repeated 30 min later. Following loading of amiodarone, a lidocaine infusion was initiated at 1  $\mu\text{g}/\text{min}$  for the remainder of the protocol. Although there was anticipated myocardial depression from this approach, there was greater concern that the porcine model has a low ventricular fibrillation threshold.

Of the 15 pigs studied, 4 died before data collection. Of the 11 remaining, complete data sets were collected for neosynephrine and aortic (Ao) occlusion. Due to ventricular fibrillation immediately after LAD occlusion, only six animals survived beyond 10 min to allow for data collection. Simulated pleural effusion was added late to the protocol and thus was only performed in the last seven pigs.

**Instrumentation overview.** Platinum-platinum black electrodes were chosen for the experiment because of their low electrode interface impedance (Medtronic, Minneapolis, MN). Electrode locations were chosen to simulate the approximate positions of biventricular leads in the RV and on the lateral LV epicardium. Two sets of four electrodes spaced 1 cm apart were sewn onto a felt backing, and each was sewn onto the LV epicardium. The anterior electrodes were sewn parallel to the distal LAD to simulate the RV lead, and the posterior electrodes were sewn parallel to a left marginal vein to simulate the LV biventricular lead. Electrode pairs were chosen for a cross-ventricular chamber tetrapolar measurement with a current-producing and a voltage-sensing electrode on both the anterior and the posterior epicardium.

The pigs were also instrumented with 2D endocardial crystals, as outlined above, a left carotid pressure sensor (3F, Scisense, London, ON), a 6F sheath in the jugular vein, an RV pressure sensor inserted directly through the anterior RV wall (1.2 F, Scisense, London, ON), a descending thoracic saline-filled balloon occluder (16- or 18-mm diameter, In Vivo Metric, Healdsburg, CA) to generate transient occlusion as an alternative method to produce LV dilation, and an Ao flow probe, which was placed in the descending thoracic aorta (Transonic, Ithaca, NY) immediately distal to the balloon occluder to document that occlusion was obtained.

**Properties measurement and hematocrit.** A custom-designed epicardial probe was applied to the surface of the intact beating open-chest heart. The stimulus current was generated using the instrumentation previously described (25). Real-time  $|\vec{Y}|$  and  $\angle \vec{Y}$  were measured, and  $\epsilon_m$  and  $\sigma_m$  were calculated, as described previously (24). Briefly, the surface probe “cell constant”,  $k$  ( $\text{m}^{-1}$ ), determined in saline of known electrical conductivity, is used to calculate:  $\sigma_m = k \times G_m$  and  $\epsilon_m = k \times C_m$ , where  $G_m = \text{Re}\{\vec{Y}\}$  and  $C_m = \text{Im}\{\vec{Y}\}/\omega$  and  $\omega = 2\pi f$ , where  $k$  is the cell constant of the probe used ( $1/\text{m}$ ),  $G_m$  is the conduc-

tance of muscle (S),  $C_m$  is the capacitance of the muscle, and  $f$  is the frequency of excitation (Hz).

Hematocrit was determined both at baseline and at the end of the experiment via capillary tubes and a Clay Adams Readacrit centrifuge (model CT-3400, Becton Dickinson, Sparks, MD). Whole blood samples were spun for 5 min at 8,500 rpm, and the volume of packed red cells was expressed as a percentage of total volume.

**Neosynephrine (phenylephrine) for LV dilatation.** Neosynephrine was chosen to increase afterload and secondarily dilate the LV in a dose-response fashion to simulate LV dilation as would occur in a HF patient. Neosynephrine was infused at a constant rate of 75, 150, and 300  $\mu\text{g}/\text{min}$  in the first two pigs. For the later nine pigs, a lower dose of 37.5  $\mu\text{g}/\text{min}$  was added to this same infusion protocol. Baseline and data from at least two doses of neosynephrine, where LV dilation occurred as defined by endocardial crystals, were required for data to be used in analysis. Some doses of neosynephrine did not result in LV dilation, and this varied in every pig. Thus the doses given in the RESULTS section are the baseline and mean low and high doses of neosynephrine that achieved LV dilation. Each dose of neosynephrine was infused for 10 min to achieve steady state, and then data were acquired over the subsequent 5 min for a total of 15 min per dose.

Data acquired included heart rate, carotid pressure [Ao pressure (AoP)], descending thoracic Ao flow, short- and long-axis endocardial crystals, epicardial impedance magnitude ( $|\vec{Z}|$ ) and phase angle ( $\angle \vec{Z}$ ). Data were acquired while the respirator was suspended at end-expiration for at least five cardiac cycles.

**Alternative methods for LV dilatation.** To determine if LV dilation could be detected by epicardial admittance, preceding an increase in RV pressures, we examined two additional preparations: acute LAD occlusion and transient Ao occlusion. The question could not be posed in the neosynephrine dose-response study, because this drug acts as an  $\alpha_2$ -receptor agonist, and this receptor is present in both the systemic and pulmonary vasculature. Thus it was not possible to obtain an isolated increase in LV afterload without a simultaneous increase in RV afterload (15, 21).

**LAD occlusion.** A suture was placed under the middle LAD, proximal to the epicardial admittance electrodes, and tied off to produce an acute dilation of the middle and distal anterior myocardium. Data obtained were identical to the neosynephrine protocol, but RV pressure was also obtained. Due to ventricular fibrillation, complete data were only obtained in six porcine studies.

**Transient Ao occlusion.** Transient Ao occlusion was performed successfully in 11 pigs. A fluid-filled saline occluder cuff controlled occlusion, and successful occlusion was defined by the reduction of descending thoracic Ao flow to  $<1$  l/min. The flow probe was always immediately distal to the balloon occluder.

**Pleural effusion simulation.** Pleural effusions are common in HF patients and are a common source of artifact in the measurement of lung conductance by systems such as Optivol (18, 31, 35) and CorVue, since the electrical fields generated by these devices extend into the lungs. Epicardial admittance generates an electric field, which extends across the LV and thus should not have this source of artifact. To test this hypothesis, the chest cavity was filled with saline during the measurement of LV epicardial admittance (both on the right and left sides of the heart). The pericardium was used as a sling to keep the saline from coming into direct contact with the electrodes, similar to the final implementation of epicardial admittance. Immediately after baseline measurements, as outlined above, saline of conductivity close to blood ( $7,941 \pm 124$   $\mu\text{S}/\text{cm}$ ) was introduced into the chest. The introduced volume for all seven pigs was  $425 \pm 90$  ml, and, following introduction, all measurements were repeated.

**Data analysis.** The slope-relating  $G_{\text{blood}}$  (mS) and endocardial crystal volume (ml) were determined in 11 animals at up to three doses of neosynephrine in each of up to six vectors, yielding a total of 99 paired measures of  $G_{\text{blood}}$  and crystal volume (Fig. 3). Data were analyzed based on a repeated-measures linear model with a compound

symmetric autocorrelation matrix and fixed intercepts for each pig and vector. The significance of the relation between  $G_{\text{blood}}$  and crystal volume was assessed using a Wald statistic for testing the null hypothesis that the coefficient of LV  $G_{\text{blood}}$  in the repeated-measures linear model is zero. Statistical testing was two-sided with a significance level of 5% using SAS version 9.2 for Windows (SAS Institute, Cary, NC). For LAD occlusion, transient Ao occlusion, and pleural effusion simulation, paired baseline and intervention data were compared using a Student's *t*-test, again with a level of significance of 5%. All results are reported as means  $\pm$  SD.

## RESULTS

### Baseline Hemodynamics

The mean systolic AoP was  $80 \pm 13$  mmHg, and the heart rate was  $86 \pm 17$  beats/min. The mean LV end-diastolic and end-systolic long axis by crystals was  $82 \pm 6$  and  $74 \pm 5$  cm, respectively; and the mean LV end-diastolic and end-systolic short axis by crystals was  $47 \pm 4$  and  $40 \pm 4$  cm, respectively. The calculated mean LV end-diastolic volume was  $100 \pm 31$  ml, and the mean LV end-systolic volume was  $69 \pm 25$  ml measured via endocardial crystals. The mean LV ejection fraction was  $31 \pm 6\%$ , consistent with a depressed but nondilated LV preparation from the anesthetics and amiodarone given to minimize ventricular fibrillation. The mean descending thoracic flow was  $8.0 \pm 1.8$  l/min, and the mean RV systolic pressure was  $19 \pm 3$  mmHg. The mean distance from the LV apex to the most apical epicardial admittance electrode on the anterior surface was  $3.0 \pm 0.9$  cm, and on the posterior surface was  $3.0 \pm 0.5$  cm, consistent with the admittance electrodes being parallel to one another on either side of the LV epicardium.

The end-diastolic and end-systolic epicardial LV admittance magnitudes ( $|\vec{Y}| = 1/|\vec{Z}|$ ) were  $15.8 \pm 2.0$  and  $14.5 \pm 1.9$  mS, respectively; and the mean  $\langle \vec{Y} = - \langle \vec{Z}$  were  $9.2 \pm 3.0$  and  $7.4 \pm 3.2^\circ$ , respectively.

### Properties Measurement and Hematocrit

Myocardial properties were determined in each pig for use in the equations to separate the blood and muscle admittance, as published previously (23). The myocardial conductivity was  $\sigma_m = 0.33 \pm 0.03$  S/m, the myocardial permittivity was  $\epsilon_m = (19,710 \pm 2,786) \times \epsilon_0$  F/m, and the calculated ratio of  $\sigma/\epsilon$  for myocardium was  $1,923,320 \pm 179,592$  S/F.

Hematocrit at the initiation of the protocol was  $30.0 \pm 2.3\%$ , and at the end of the protocol  $33.0 \pm 4.7\%$ , consistent with hemoconcentration due to minimal fluid administration during the protocol to mitigate changes in blood and myocardial electrical properties as a source of artifact.

### Neosynephrine for LV Dilatation

Example data are shown in Fig. 2, which demonstrates that the short- and long-axis crystals used to derive the standard for LV volume, and the  $|\vec{Z}|$  and  $\langle \vec{Z}$  used to derive LV  $G_{\text{blood}}$  both detected dose-by-dose LV dilation. Data from 11 porcine studies are shown in Fig. 3. The low-dose neosynephrine was  $90 \pm 54$   $\mu\text{g}/\text{min}$ , the high-dose neosynephrine was  $180 \pm 107$   $\mu\text{g}/\text{min}$ . The  $G_{\text{blood}}$  was computed from the  $|\vec{Z}|$  and  $\langle \vec{Z}$ , and plotted against LV volume calculated from endocardial crystals. LV end-diastolic volume and complex impedance at end

diastole were measured in each pig, and the results were converted into the  $G_{\text{blood}}$  (LV  $G_{\text{blood}}$ ) using the admittance technique, removing muscle contribution in real time (Fig. 3A). The  $G_{\text{blood}}$ , expressed in milliSiemens (mS), and LV volume, expressed in milliliters (ml), were measured at multiple values of LV volume for between one and six vectors on each pig, and the within-animal mean slope was computed for Fig. 3A. The slope relating  $G_{\text{blood}}$  (mS) and the adjusted volume (ml),  $1.16 \pm 0.48$  mS/ml, was significantly different from zero ( $P = 0.017$ ). Data were also analyzed using the traditional conductance technique, which does not remove muscle contribution and demonstrates that our ability to detect LV dilation was lost and is dependent on having access to the imaginary component of the myocardial signal (Fig. 3B).

### LAD Occlusion for LV Dilatation

Hemodynamic parameters are shown in Table 1 at baseline and following LAD occlusion. Acute LAD occlusion produced a significant decrease in AoP and Ao flow. The anticipated increase in LV volume was detected by both the standard (endocardial crystals), as well as  $G_{\text{blood}}$ . The large standard deviations in the  $G_{\text{blood}}$  are a result of the wide range of electrode positions and an offset, which may be caused by variable surface electrode-myocardium contact. On average, an increase of 17% from baseline LV  $G_{\text{blood}}$  corresponded to an LV volume increase of 4%.

### Transient Ao Occlusion

Hemodynamic parameters are shown in Table 2 at baseline and peak transient Ao occlusion. AoP and endocardial crystal-derived LV volume both increased. Ao flow decreased  $<1$  l/min because that was the definition for a successful Ao occlusion. The increased afterload increases the LV  $G_{\text{blood}}$  by 7% and the crystal LV volume by 9%. RV systolic pressure also increased slightly.

### Pleural Effusion Simulation

Hemodynamic parameters are shown in Table 3 at baseline and during pleural effusion simulation. Neither the LV  $G_{\text{blood}}$  nor the crystal-derived LV volume changed with saline placed around the heart.

## DISCUSSION

This study has demonstrated that LV  $G_{\text{blood}}$  can be determined from the epicardial position, despite the current gener-

Table 1. Left anterior descending coronary artery occlusion

	Baseline	Occlusion
HR, beats/min	$88 \pm 19$	$87 \pm 20$
AoP, mmHg	$88 \pm 9$	$83 \pm 11^*$
Crystal volume, ml	$88 \pm 12$	$91 \pm 12^*$
Ao flow, l/min	$7.0 \pm 1.3$	$6.4 \pm 1.3^*$
RVSP, mmHg	$24.5 \pm 3.9$	$23.7 \pm 5$
$G_{\text{blood}}$ , mS	$73.6 \pm 39.8$	$85.0 \pm 51.1^*$

Values are means  $\pm$  SD from 6 pigs from 13 electrode positions. HR, heart rate; AoP, systolic right carotid (aortic) pressure; crystal volume, two-dimensional endocardial crystal left ventricular volume; Ao flow, descending thoracic aortic flow; RVSP, right ventricular systolic pressure;  $G_{\text{blood}}$ , left ventricular blood conductance derived from epicardial admittance.  $*P < 0.01$ .

Table 2. *Transient Ao occlusion*

	Baseline	Occlusion
HR, beats/min	90 ± 28	97 ± 24
AoP, mmHg	86 ± 11	124 ± 18*
Crystal volume, ml	89 ± 21	98 ± 22*
Ao flow, l/min	6.3 ± 1.2	0.7 ± 0.6*
RVSP, mmHg	22.9 ± 4.4	23.8 ± 4.4*
G <sub>blood</sub> , mS	53.5 ± 18.6	57.4 ± 21.6*

Values are means ± SD from 11 pigs from 27 electrode positions. Occlusion data were defined at the time of peak AoP. \* $P < 0.01$ .

ating and sensing electrodes being in constant motion with the heart, and with dynamic removal of the myocardial component of the returning voltage signal. Specifically, it has been demonstrated that 1) a physiological LV G<sub>blood</sub> signal can be derived; 2) LV dilation in response to dose-response intravenous neosynephrine can be detected by G<sub>blood</sub> in a similar fashion to the standard of endocardial crystals when admittance is used, but not when only traditional conductance is used; 3) the physiological impact of acute LAD occlusion and resultant LV dilation can be detected by G<sub>blood</sub>, before the anticipated secondary rise in RV systolic pressure; and 4) a pleural effusion simulated by placing saline outside the pericardium does not serve as a source of artifact for G<sub>blood</sub> measurements.

Epicardial admittance tracks endocardial crystal-derived volumes accurately. We have demonstrated, via a repeated-measures linear model, an increase in the mean admittance volume with the standard of endocardial crystal volume with neosynephrine dose, and significant variation in the relation between mean admittance volume and endocardial crystal volume with dose ( $P < 0.001$ ), reflecting greater changes in admittance volume with dose for larger hearts. The implication is that the admittance technique becomes more robust at detecting LV dilation in the largest hearts. The further advantage of the new technique is that it provides a measure of LV volume (G<sub>blood</sub>) that can be safely translated to patients with HF, since it makes no changes to the electrodes currently implanted. Rather, it can be implemented through firmware and hardware changes to the existing circuit incorporated in the case of the generator of currently implanted AICD/biventricular pacemakers.

Right-sided pressures are used in many implanted devices to predict future episodes of HF in patients (1, 7, 19, 27). The backwards HF theory (8) argues that HF initiates in the LV in these patients and subsequently elevates left atrial pressure, resulting in pulmonary edema, and finally elevates right-sided pressures, all subsequent to LV volume or preload and hence less sensitive measures of future HF episodes. This theory is best tested in a chronic HF model, since LV diastolic compli-

Table 3. *Pleural effusion simulation*

	Baseline	Pleural Effusion
HR, beats/min	95 ± 19	96 ± 21†
AoP, mmHg	87 ± 5	86 ± 6*
Crystal volume, ml	100 ± 29	100 ± 27
G <sub>blood</sub> , mS	53.2 ± 33.5	52.6 ± 27.8

Values are means ± SD from 7 pigs from 54 electrode positions. † $P < 0.05$ , \* $P < 0.01$ .

ance is increased by this condition, and hence a greater change in LV volume will produce a less robust elevation of right-sided pressures. Despite our study being an acute preparation examining normal-sized LVs (even considering depression of ventricular function by amiodarone and anesthetics), acute LAD occlusion was able to confirm this theory by demonstrating an elevation of both LV G<sub>blood</sub> and echo crystal volume, but no increase in RV systolic pressures. These results are consistent with our hypothesis that an increasing LV G<sub>blood</sub> will be a more sensitive indicator of impending future episodes of HF than alternative pressure and lung conductance approaches.

Pleural effusions are frequent findings in patients with advanced HF. Devices that interrogate the lungs for pulmonary edema use a transthoracic resistance measurement from the tip of the RV lead to the case of the battery pack for the pacemaker/defibrillator and thus provide a wide electric field encompassing the LV, left atrium, thoracic skeletal muscle, ipsilateral lung tissue, intravascular blood volume in the lung, pulmonary interstitial edema, and finally pleural effusions to measure a changing fluid index. Having an electrical approach that is focused on the LV myocardium and blood volume would be preferable, but there still exists some electrical field extension into other sources of artifact, such as pleural effusions. To determine whether epicardial admittance would artifactually detect pleural effusions, we placed fluid outside the pericardium in the chest cavity to simulate this clinical condition. We demonstrate no alteration in the measurement of LV G<sub>blood</sub> in our studies, implying that epicardial admittance does indeed focus its interrogation on the LV itself.

The admittance technique (Fig. 3A) provides reliable tracking of LV preload similar to endocardial crystals, whereas traditional conductance does not (Fig. 3B). This increased sensitivity of the admittance technique is due to the use of a phase measurement in the calculation of the admittance, which allows the real-time separation of blood and muscle components. The high resistance of muscle normally swamps a measurement of blood and muscle in series, because the resistivity of muscle is nearly five times that of blood. This causes the total measured traditional conductance signal to be low and nonspecific (Fig. 3B) compared with the LV G<sub>blood</sub> determined using admittance (Fig. 3A).

In contradiction, studies by Stahl et al. (28, 29), using traditional conductance, have shown promise in the detection of HF using existing biventricular leads. The study of Stahl et al. is very different from the present study for two reasons. The first major difference is that our stimulating electrodes span the LV, whereas, in Stahl's, they reside completely within the RV. In Stahl's design, the majority of current will be confined to the

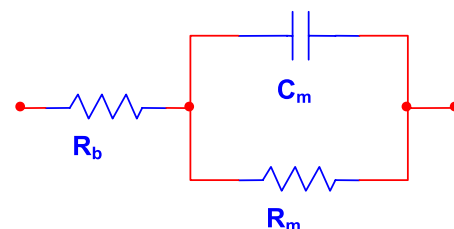


Fig. 4. Circuit model for epicardial admittance measurement. R<sub>b</sub>, resistance of blood; R<sub>m</sub>, resistance of muscle; C<sub>m</sub>, capacitance of the muscle.

RV because the resistivity of muscle is five times higher than blood. This limitation is overcome in the present study by forcing the current across the LV by maintaining the current electrodes on opposite sides of the LV. The preferential path for current is, therefore, the low-resistivity blood pool. The second major difference is that the present study employs complex admittance for determining the relative muscle contribution to the measured signal. As seen in Fig. 3, this separation of blood from muscle provides increased sensitivity to HF detection (increasing LV preload). Our study represents the first evidence that a cross-chamber complex admittance measurement shows improved sensitivity to LV blood pool volume measurement over a traditional conductance (or resistance) measurement.

There are several limitations of our study. First, although we were able to distinguish an increase in LV volume from RV systolic pressure with LAD occlusion, we were unable to do so for transient Ao occlusion. However, while RV systolic pressure increase was statistically significant with transient Ao occlusion, the absolute mean increase was 0.9 mmHg, which is not clinically significant. We could not use neosynephrine infusion to test the theory that LV preload will be a more sensitive indicator of impending HF than right-sided pressures, since both the systemic and pulmonary circuits have  $\alpha_2$ -receptors (15, 21). Ultimately, this theory is best tested in a dilated LV, where reduced chamber compliance will further favor LV preload as being the most sensitive endpoint for impending HF than pressure measurement. Second, we did not place the admittance electrodes onto ACID and biventricular pacing leads deployed in their recommended locations. However, we anticipate that, as the technique transitions to a closed-chest preparation in future embodiments of this technology, there will be improved admittance electrode contact, which was a source of error in the present study due to air acting as an insulator between the electrode-myocardial interface in the open-chest porcine preparation. This will substantially change the electrode interface impedance. It is anticipated that this source of artifact will no longer be relevant, as our approach transitions into a closed-chest preparation. Third, due to biological variation, not every dose of neosynephrine produced dilation in LV chamber volume. Since the end point of our study was LV dilation, only data from those neosynephrine doses that resulted in LV dilation were included in data analysis. Finally, although LV  $G_{\text{blood}}$  can be used as a surrogate to volume, we did not actually convert LV  $G_{\text{blood}}$  to LV volume. The equation of Baan et al. (3, 4) is not applicable, since  $L$  is not a constant with epicardial electrode placement. Future studies will benefit from derivation of a new  $G_{\text{blood}}$  to LV volume equation.

In conclusion, we have developed a new electrical approach to impending HF detection, taking advantage of preexisting AICD and biventricular pacing lead locations, and maturing the conductance approach to moving source and sensing electrodes, while instantaneously removing the myocardial component to generate a final LV  $G_{\text{blood}}$  signal.

## APPENDIX

The blood and myocardium affect the electric field generated from the epicardial position differently than in the traditional intraventricular fixed electrode catheter measurement. In the epicardial lead configuration, the field travels completely through the entire thickness

of the myocardial wall on both sides of the LV, while, in an intraventricular configuration, only a part of the field enters the myocardium (i.e., traditional parallel conductance). This dictates the evolution of a unique circuit model to explain the new electrode position. The real part of the impedance  $|\vec{Z}|$  (more commonly known by its inverse, traditional conductance), is used to determine LV volume from the intraventricular position by creating a circuit model of the blood and muscle resistance in parallel. This traditional approach has not included the capacitance of the myocardium, introduced by our laboratory's admittance approach (23). In contrast, the circuit model used in the epicardial approach introduced in the present study is both a series and a parallel combination (see Fig. 4). The capacitive component of the myocardium is in parallel with the muscle resistance. Furthermore, the blood resistance is now in series with the parallel muscle resistive and capacitive components, leading to different equations for dynamic separation of blood and muscle components.

The equations for separating  $R_m$  and  $R_b$  are derived using basic circuit theory from the model presented in Fig. 4.

The equation describing this circuit is as follows:

$$\vec{Z} = \left[ R_b + \frac{R_m}{1 + (\omega R_m C_m)^2} - i \frac{(\omega R_m^2 C_m)}{1 + (\omega R_m C_m)^2} \right]$$

where  $\omega$  is the angular frequency ( $\omega = 2\pi f$ ). As can be seen in the above equation, the blood ( $R_b$ ) and muscle ( $R_m$ ) components are separable, using the previously described conductance/capacitance relationship (23).

## GRANTS

This study was supported in part by National Institutes of Health Grant R21 HL 079926, Grant UL 1RR025767 from the National Center for Research Resources, and grants from the University of Texas Health Science Center in San Antonio (Biscoe Division of Cardiology and South Texas Technology Management). Research was funded in part by a grant given by Medtronic Corporation (Minneapolis, MN).

## DISCLOSURES

No conflicts of interest, financial or otherwise, are declared by the author(s).

## REFERENCES

1. Adamson PB, Magalski A, Braunschweig F, Bohm M, Reynolds D, Steinhaus D, Luby A, Linde C, Ryden L, Cremers B, Takle T, Bennett T. Ongoing right ventricular hemodynamics in heart failure: clinical value of measurements derived from an implantable monitoring system. *J Am Coll Cardiol* 41: 565–571, 2003.
2. Baan J, Jong TT, Kerkhof PL, Moene RJ, van Dijk AD, van der Velde ET, Koops J. Continuous stroke volume and cardiac output from intraventricular dimensions obtained with impedance catheter. *Cardiovasc Res* 15: 328–334, 1981.
3. Baan J, Jong TTA, Kerkhof PLM, Moene RJ, Vandijk AD, Vandervelde ET, Koops J. Continuous stroke volume and cardiac-output from intraventricular dimensions obtained with impedance catheter. *Cardiovasc Res* 15: 328–334, 1981.
4. Baan J, Vandervelde ET, Debruin HG, Smeenk GJ, Koops J, Vandijk AD, Temmerman D, Senden J, Buis B. Continuous measurement of left-ventricular volume in animals and humans by conductance catheter. *Circulation* 70: 812–823, 1984.
5. Bardy GH, Lee KL, Mark DB, Poole JE, Packer DL, Boineau R, Domanski M, Troutman C, Anderson J, Johnson G, McNulty SE, Clapp-Channing N, Davidson-Ray LD, Fraulo ES, Fishbein DP, Luceri RM, Ip JH. Amiodarone or an implantable cardioverter-defibrillator for congestive heart failure. *N Engl J Med* 352: 225–237, 2005.
6. Bleumink GS, Knetsch AM, Sturkenboom MC, Straus SM, Hofman A, Deckers JW, Witteman JC, Stricker BH. Quantifying the heart failure epidemic: prevalence, incidence rate, lifetime risk and prognosis of heart failure. The Rotterdam Study. *Eur Heart J* 25: 1614–1619, 2004.
7. Bourge RC, Abraham WT, Adamson PB, Aaron MF, Aranda JM Jr, Magalski A, Zile MR, Smith AL, Smart FW, O'Shaughnessy MA,

- Jessup ML, Sparks B, Naftel DL, Stevenson LW. Randomized controlled trial of an implantable continuous hemodynamic monitor in patients with advanced heart failure: the COMPASS-HF study. *J Am Coll Cardiol* 51: 1073–1079, 2008.
8. Braunwald E. *Braunwald's Heart Disease. A Textbook of Cardiovascular Medicine*. Philadelphia, PA: Saunders, 2005, p. 540.
  9. Bristow MR, Saxon LA, Boehmer J, Krueger S, Kass DA, De Marco T, Carson P, DiCarlo L, DeMets D, White BG, DeVries DW, Feldman AM. Cardiac-resynchronization therapy with or without an implantable defibrillator in advanced chronic heart failure. *N Engl J Med* 350: 2140–2150, 2004.
  10. Cleland JG, Coletta AP, Clark AL, Velavan P, Ingle L. Clinical trials update from the European Society of Cardiology Heart Failure meeting and the American College of Cardiology: darbepoetin alfa study, ECHOS, and ASCOT-BPLA. *Eur J Heart Fail* 7: 937–939, 2005.
  11. Cleland JG, Daubert JC, Erdmann E, Freemantle N, Gras D, Kappenberger L, Tavazzi L. The effect of cardiac resynchronization on morbidity and mortality in heart failure. *N Engl J Med* 352: 1539–1549, 2005.
  12. Faes TJ, van der Meij HA, de Munck JC, Heethaar RM. The electric resistivity of human tissues (100 Hz–10 MHz): a meta-analysis of review studies. *Physiol Meas* 20: R1–R10, 1999.
  13. Feldman MD, Erikson JM, Mao Y, Korcarz CE, Lang RM, Freeman GL. Validation of a mouse conductance system to determine LV volume: comparison to echocardiography and crystals. *Am J Physiol Heart Circ Physiol* 279: H1698–H1707, 2000.
  14. Gaynor JW, Feneley MP, Gall SA Jr, Maier GW, Kisslo JA, Davis JW, Rankin JS, Glower DD Jr. Measurement of left ventricular volume in normal and volume-overloaded canine hearts. *Am J Physiol Heart Circ Physiol* 266: H329–H340, 1994.
  15. Glusa E, Markwardt F. Characterisation of postjunctional alpha-adrenoceptors in isolated human femoral veins and arteries. *Naunyn Schmiedeberg Arch Pharmacol* 323: 101–105, 1983.
  16. Graham MR, Warrion RK, Girling LG, Doiron L, Lefevre GR, Cheang M, Mutch WA. Fractal or biologically variable delivery of cardioplegic solution prevents diastolic dysfunction after cardiopulmonary bypass. *J Thorac Cardiovasc Surg* 123: 63–71, 2002.
  17. Lainchbury JG, Meyer DM, Jougasaki M, Burnett JC Jr, Redfield MM. Effects of adrenomedullin on load and myocardial performance in normal and heart-failure dogs. *Am J Physiol Heart Circ Physiol* 279: H1000–H1006, 2000.
  18. Luthje L, Drescher T, Zenker D, Vollmann D. Detection of heart failure decompensation using intrathoracic impedance monitoring by a triple-chamber implantable defibrillator. *Heart Rhythm* 2: 997–999, 2005.
  19. Magalski A, Adamson P, Gadler F, Boehm M, Steinhaus D, Reynolds D, Vlach K, Linde C, Cremers B, Sparks B, Bennett T. Continuous ambulatory right heart pressure measurements with an implantable hemodynamic monitor: a multicenter, 12-mo follow-up study of patients with chronic heart failure. *J Card Fail* 8: 63–70, 2002.
  20. Moss AJ, Zareba W, Hall WJ, Klein H, Wilber DJ, Cannom DS, Daubert JP, Higgins SL, Brown MW, Andrews ML. Prophylactic implantation of a defibrillator in patients with myocardial infarction and reduced ejection fraction. *N Engl J Med* 346: 877–883, 2002.
  21. Pepke-Zaba J, Higenbottam TW, Dinh-Xuan AT, Riddon C, Kealey T. Alpha-adrenoceptor stimulation of porcine pulmonary arteries. *Eur J Pharmacol* 235: 169–175, 1993.
  22. Porterfield JE, Kottam AT, Raghavan K, Escobedo D, Jenkins JT, Larson ER, Trevino RJ, Valvano JW, Pearce JA, Feldman MD. Dynamic correction for parallel conductance,  $g_p$ , and gain factor,  $\alpha$ , in invasive murine left ventricular volume measurements. *J Appl Physiol* 107: 1693–1703, 2009.
  23. Raghavan K, Kottam AT, Valvano JW, Pearce JA. Design of a wireless telemetric backpack device for real-time in vivo measurement of pressure-volume loops in conscious ambulatory rats. *Conf Proc IEEE Eng Med Biol Soc* 2008: 993–996, 2008.
  24. Raghavan K, Porterfield JE, Kottam AT, Feldman MD, Escobedo D, Valvano JW, Pearce JA. Electrical conductivity and permittivity of murine myocardium. *IEEE Trans Biomed Eng* 56: 2044–2053, 2009.
  25. Raghavan K, Wei CL, Kottam A, Altman DG, Fernandez DJ, Reyes M, Valvano JW, Feldman MD, Pearce JA. Design of instrumentation and data-acquisition system for complex admittance measurement. *Biomed Sci Instrum* 40: 453–457, 2004.
  26. Reyes M, Steinhelper ME, Alvarez JA, Escobedo D, Pearce J, Valvano JW, Pollock BH, Wei CL, Kottam A, Altman D, Bailey S, Thomsen S, Lee S, Colston JT, Oh JH, Freeman GL, Feldman MD. Impact of physiological variables and genetic background on myocardial frequency-resistivity relations in the intact beating murine heart. *Am J Physiol Heart Circ Physiol* 291: H1659–H1669, 2006.
  27. Rozenman Y, Schwartz RS, Shah H, Parikh KH. Wireless acoustic communication with a miniature pressure sensor in the pulmonary artery for disease surveillance and therapy of patients with congestive heart failure. *J Am Coll Cardiol* 49: 784–789, 2007.
  28. Stahl C, Beierlein W, Walker T, Straub A, Nagy Z, Knubben K, Greiner TO, Lippert M, Czygan G, Paule S, Schweika O, Kuhlkamp V. Intracardiac impedance monitors hemodynamic deterioration in a chronic heart failure pig model. *J Cardiovasc Electrophysiol* 18: 985–990, 2007.
  29. Stahl C, Walker T, Straub A, Kettering K, Knubben K, Greiner TO, Paule S, Lippert M, Czygan G, Schweika O, Kuhlkamp V. Assessing acute ventricular volume changes by intracardiac impedance in a chronic heart failure animal model. *Pacing Clin Electrophysiol* 32: 1395–1401, 2009.
  30. Steendijk P, van der Velde ET, Baan J. Dependence of anisotropic myocardial electrical resistivity on cardiac phase and excitation frequency. *Basic Res Cardiol* 89: 411–426, 1994.
  31. Vollmann D, Nagele H, Schauer P, Wiegand U, Butter C, Zanotto G, Quesada A, Guthmann A, Hill MR, Lamp B. Clinical utility of intrathoracic impedance monitoring to alert patients with an implanted device of deteriorating chronic heart failure. *Eur Heart J* 28: 1835–1840, 2007.
  32. Wang L, Lahtinen S, Lentz L, Rakov N, Kaszas C, Ruetz L, Stylos L, Olson WH. Feasibility of using an implantable system to measure thoracic congestion in an ambulatory chronic heart failure canine model. *Pacing Clin Electrophysiol* 28: 404–411, 2005.
  33. Wei CL, Valvano JW, Feldman MD, Nahrendorf M, Peshock R, Pearce JA. Volume catheter parallel conductance varies between end-systole and end-diastole. *IEEE Trans Biomed Eng* 54: 1480–1489, 2007.
  34. Wei CL, Valvano JW, Feldman MD, Pearce JA. Nonlinear conductance-volume relationship for murine conductance catheter measurement system. *IEEE Trans Biomed Eng* 52: 1654–1661, 2005.
  35. Yu CM, Wang L, Chau E, Chan RH, Kong SL, Tang MO, Christensen J, Stadler RW, Lau CP. Intrathoracic impedance monitoring in patients with heart failure: correlation with fluid status and feasibility of early warning preceding hospitalization. *Circulation* 112: 841–848, 2005.